Eur J Nucl Med Mol Imaging (2016) 43:1621–1629
DOI 10.1007/s00259-016-3345-1

ORIGINAL ARTICLE

RGD-K5 PET/CT in patients with advanced head and neck cancer treated with concurrent chemoradiotherapy: Results from a pilot study

Shih-Hsin Chen[1] · Hung-Ming Wang[2] · Chien-Yu Lin[3] · Joseph Tung-Chieh Chang[3] · Chia-Hsun Hsieh[2] · Chun-Ta Liao[4] · Chung-Jan Kang[4] · Lan-Yan Yang[5] · Tzu-Chen Yen[1]

Received: 9 November 2015 / Accepted: 16 February 2016 / Published online: 27 February 2016

Abstract
Background/Aim We prospectively investigated the potential usefulness of PET using a new tracer targeting integrin αvβ3 (termed RGD-K5) in patients with head and neck cancer (HNC) undergoing definitive concurrent chemoradiotherapy (CCRT).
Patients and Methods Newly diagnosed patients with locally advanced HNC scheduled for definitive CCRT were eligible. RDG-K5 PET and FDG PET scans were performed at three different time points (baseline, 2 weeks, and 3 months post-treatment).
Results Nine patients completed all of the three scans, whereas two patients withdrew after two scans only. Uptake of both RGD-K5 and FDG generally decreased following CCRT. However, the observed decrease did not differ significantly between complete responders and non-responders. At 3 months post-treatment, the uptake of both RGD-K5 and FDG at the main tumors was significantly lower in those who achieved complete responses than in those with residual tumors.
Conclusion RGD-K5 PET has the potential to identify patients with incomplete responses to CCRT.

Keywords RGD-K5 · Integrin αvβ3 · FDG · PET · Head and neck cancer · CCRT

Chung-Jan Kang is co-first author.

✉ Tzu-Chen Yen
yen1110@adm.cgmh.org.tw

[1] Department of Nuclear Medicine, Chang-Gung Memorial Hospital, Linkou, 5, Fu-Shin St., Kwei-Shan Township, TaoYuan County, Taiwan 333

[2] Division of Hematology/Oncology, Department of Internal Medicine, Chang-Gung Memorial Hospital, Linkou, 5, Fu-Shin St., Kwei-Shan Township, TaoYuan County, Taiwan 333

[3] Department of Radiation Oncology, Chang-Gung Memorial Hospital, Linkou, 5, Fu-Shin St., Kwei-Shan Township, TaoYuan County, Taiwan 333

[4] Departments of Otorhinolaryngology, Head and Neck Surgery, Chang-Gung Memorial Hospital, Linkou, 5, Fu-Shin St., Kwei-Shan Township, TaoYuan County, Taiwan 333

[5] Clinical Trial Center, Chang-Gung Memorial Hospital, Linkou, 5, Fu-Shin St., Kwei-Shan Township, TaoYuan County, Taiwan 333

Introduction

Angiogenesis, defined as the formation of new blood vessels by a process of sprouting from pre-existing vessels, is a hallmark of malignant tumor progression [1]. Integrins, a family of transmembrane glycoprotein receptors that mediate cell-matrix adhesion, have been shown to play a major role in cell migration, invasion, and proliferation. Integrins are heterodimers of non-covalently associated α- and β-subunits (18 α-subunits and eight β-subunits). A high expression of integrin αvβ3 has been reported in tumor-associated blood vessels, where it may promote angiogenesis and tumor invasion [2]. In particular, integrin αvβ3 has been found to be involved in endothelial cell proliferation and new blood vessel formation in head and neck malignancies [3]. A previous positron emission tomography (PET) study has shown that integrin αvβ3 expression can be traced using F-18 Galacto-RGD [4]. Notably, this imaging modality has been successfully used to identify integrin αvβ3 in the neovasculature of patients with head and neck squamous cell carcinomas [5].

Patients with locally advanced head and neck cancer (HNC) usually receive definitive concurrent chemoradiotherapy

(CCRT) for considerations of functioning preservation or unresectable diseases [6]. Unfortunately, the outcomes were dismal, the 5-year overall survival rate being < 50 % [7]. Recent advances in drug development allowed the inclusion of anti-angiogenic drugs in standard treatment regimens. However, the ideal target population for anti-angiogenic therapy of head and neck tumors has not been clearly identified. In this scenario, we designed a prospective pilot study to investigate the potential clinical usefulness of PET using a new tracer that specifically targets integrin αvβ3 (termed RGD-K5) in patients with locally advanced HNC treated with definitive CCRT.

Materials and Methods

Ethics

Ethical approval was granted by the Institutional Review Boards of the Chang Gung Memorial Hospital (99-3338A) and the Department of Health, Executive Yuan, Taiwan. The study was registered at clinicaltrials.gov (NCT01447134). All participants gave their written informed consent before inclusion in the study.

Patients

Patients with biopsy-proven HNC who were scheduled to receive CCRT between June 2013 and April 2014 were deemed eligible. According to our institutional guidelines, all patients were staged with magnetic resonance imaging (MRI) and FDG PET. The baseline RGD-K5 PET scan was scheduled within 2 weeks of conventional imaging for staging purposes. Two additional FDG PET and RGD-K5 PET scans were planned at 2 weeks and 3 months post CCRT. All participants were followed for at least 12 months or censored on the date of death. The ability of the two tracers to distinguish between patients who were successfully treated and those with residual disease served as the main outcome measure.

RGD-K5 PET imaging

RGD-K5 was synthesized according to the instructions provided by Siemens [8]. At 60 min after a single bolus intravenous injection of 10 mCi RGD-K5, whole-body static PET images were acquired from the skull base to the thigh. Imaging was performed on a Siemens Biograph mCT scanner (Siemens Medical Solutions, Malvern, PA, USA), with an acquisition time of 2 min for each bed position. Non-contrast CT data were acquired for anatomical correlation and attenuation correction. The tracer uptake was quantified using the standardized uptake value (SUV) calculated as tissue concentration (Bq/g)/[injected dose (Bq)/body weight (g)].

FDG PET imaging

Patients were required to fast for at least 4 h before FDG PET imaging in order to achieve a plasma glucose level < 200 mg/dL. At 60 min after the intravenous injection of 10 mCi FDG, whole-body static PET images were acquired from the skull base to the thigh. Imaging was performed on a Siemens Biograph mCT scanner (Siemens Medical Solutions), with an acquisition time of 2 min for each bed position. Non-contrast CT data were acquired for anatomical correlation and attenuation correction.

Treatment and follow-up

All of the patients were treated with intensity-modulated radiotherapy with a 6-MV X-ray at 2 Grays (Gy) per fraction, with five fractions per week. The radiation dose was 46–50 Gy for all subclinical risk areas, including the neck lymphatics, and 72 Gy for the primary tumor and grossly involved nodal disease. Concurrent chemotherapy consisted of cisplatin 50 mg/m^2 on day 1, and oral tegafur 800 mg/day plus leucovorin 60 mg/day from day 1 to day 14. The scheme was repeated every 2 weeks through the radiotherapy course [9].

Following treatment, the patients were followed up by physical examination and fiberoptic pharyngoscopy every 1 to 3 months. MRI was performed 3 months after completion of treatment, and additional MRI or CT scans were performed every 6 months thereafter or in the presence of clinical deterioration. Biopsy was performed for any suspicious residual/recurrent tumors whenever possible. If biopsy was not feasible, close clinical and imaging follow-up was pursued. All patients were followed up for at least 12 months after treatment or until death.

Statistical analysis

Continuous data were compared using the Student's *t*-test and Wilcoxon signed-rank test for independent-group comparison and matched pair comparison, respectively. The Spearman's rank correlation coefficient (ρ) was used to investigate the associations between the study variables. Power analysis was calculated with G*Power software (version 3.1.5) [10]. All other calculations were performed using the SPSS 16.0 statistical package (SPSS Inc., Chicago, IL, USA). Two-tailed p values < 0.05 were considered statistically significant.

Results

Patient characteristics

A total of 17 patients with written informed consent were included; however, six of them voluntarily withdrew and

two refused the final post-treatment scan. Consequently, nine patients who had completed all three scans and two patients with two sets of scans were included in the analysis. One patient had synchronous cancers, and thus both primary lesions were analyzed. The general characteristics of the study participants are shown in Table 1. All patients were followed for at least 12 months, the only exception being a patient who died 326 days after the initial RGD-K5 PET scan. The median follow-up time for the entire cohort was 664 days (range: 326–766 days).

At 3 months post-treatment evaluation, two patients had persistent main tumors, three had nodal disease, and one had both of them. All patients were pathologically proven. In addition, all underwent salvage surgery, the only exception being one patient who received palliative chemotherapy. Three of those who received salvaged surgery were disease-free, whereas two continued to present lymph node recurrences (one of them eventually died of disease).

The remaining five patients were free of disease following CCRT. However, the patient with synchronous cancers developed a third primary esophageal neoplasm; he eventually died of esophageal cancer. Another participant developed distant bone metastases 477 days after CCRT (Fig. 1).

The FDG and RGD-K5 images of a representative patient are shown in Fig. 2.

Baseline RGD-K5 and FDG uptake

The main tumor and nodal RGD-K5 and FDG uptakes according to different treatment outcomes are summarized in Tables 2, 3, and 4. The modifications in RGD-K5 and FDG uptake (compared with baseline values and expressed using the SUV) at 2 weeks and 3 months post-treatment are depicted in Figs. 3 and 4, respectively. At baseline scans, no significant differences in the mean RGD-K5 uptake were noted between patients who had tumor complete remission or not (main tumor: 5.6 *versus* 5.1, respectively, $p = 0.746$; lymph nodes: 4.7 versus 3.7, respectively, $p = 0.663$). Similarly, the mean baseline FDG uptake did not differ significantly between responders and non-responders, either (main tumor: 15.1 versus 15.9, respectively, $p = 0.753$; lymph nodes: 12.3 versus 11.2, respectively, $p = 0.647$).

CCRT-induced changes in RGD-K5 uptake

At 2 weeks post-treatment, the RGD-K5 uptake did not differ significantly between those who achieved complete remission compared with those who did not (main tumor SUV: 3.6 versus 4.7, respectively, $p = 0.163$; lymph nodes SUV: 2.3 versus 2.8, respectively, $p = 0.227$). The difference in RGD-K5 uptake was calculated from baseline. The changes of RGD-K5 uptake compared to baseline varied from −75 % to +80 % (mean: −13 %, $p = 0.117$) for the main tumors and from

Table 1 General characteristics of the study patients

Patient no.	Age, years	Sex	Main tumor site	Staging	Definitive Treatment	Follow-up (months)	Recurrence (months‡)	Salvage treatment	Double cancer/primary	Outcomes (months‡)
1	55	M	Tonsil/ Retromolar	T3N1/ T2N0	CCRT	24.4	–	–	Third primary: esophageal cancer	Died* (20.8)
2	49	M	Hypopharynx	T4aN2b	CCRT	24.6	T+N (2.7)	Surgery	Double: gingival cancer	NED
3	48	M	Hypopharynx	T3N2b	CCRT	25.8	–	–	–	NED
4	42	M	Nasopharynx	T3N1	CCRT	24.4	N (3.7)	Surgery	–	AWD
5	61	M	Tonsil	T2N2b	CCRT	23.9	Iliac bone metastases (15.9)	Chemotherapy +RT (long-term palliation)	–	AWD
6	43	M	Hypopharynx	T3N2b	CCRT	11.5	N (3.8)	Surgery	–	Died† (8.6)
7	49	M	Tonsil	T3N2b	CCRT	23.9	N (4.5)	Surgery	–	NED
8	47	M	Tonsil	T4aN3	CCRT	20.6	–	–	–	NED
9	54	M	Hypopharynx	T4bN3	CCRT	16.3	–	–	–	NED
10	53	M	Buccal	T4bN2c	CCRT	16.6	T (8.5)	Palliation	–	AWD
11	55	M	Larynx	T4aN0	CCRT	17.6	T (9.1)	Surgery	–	NED

* Died of esophageal cancer

† Died of septic shock/pneumonia during palliative chemotherapy

‡ Calculated from the end of CCRT

Abbreviations: M, male; CCRT, concurrent chemoradiotherapy; T, main tumor; N, lymph nodes; NED, no evidence of disease; AWD, alive with disease

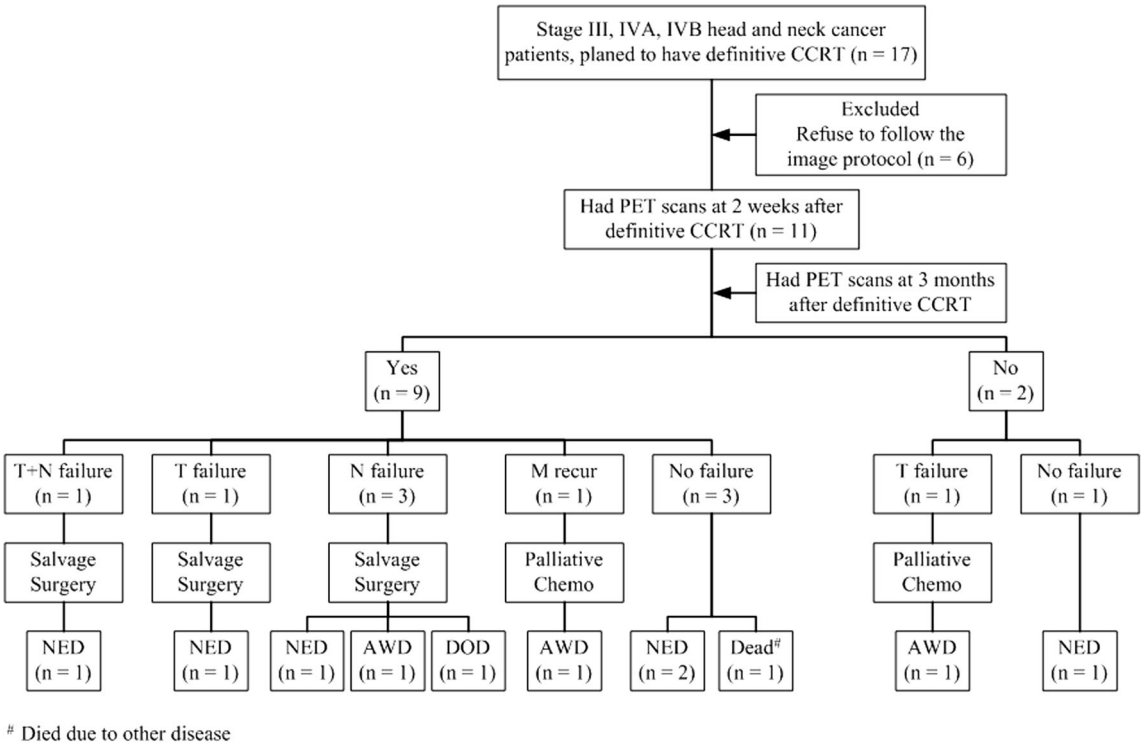

Fig. 1 Flow chart of the participants through the study and main clinical outcomes. Abbreviations: CCRT, concurrent chemoradiotherapy; T, main tumor; N, lymph nodes; NED, no evidence of disease; AWD, alive with disease; DOD, died of other diseases

−75 % to +13 %, (mean: −27 %, $p=0.037$) for nodes. The observed decrease did not differ significantly between patients whose main tumor achieved complete remission versus those who did not (−15 % versus −7 %, respectively, $p=0.806$). Similar observations were observed for the decrease in nodal uptake (−35 % versus −15 %, respectively, $p=0.320$).

At 3-month post-treatment scan, the mean SUV of the main tumors was significantly lower in patients whose main tumor showed a complete remission compared with those who did not (2.6 versus 3.9, respectively, $p=0.007$); the estimated power achieved 88.8 % under significance level 0.05. The mean SUV of lymph nodes did not differ significantly between responders and non-responders (2.0 versus 2.6, respectively, $p=0.293$). Compared with baseline, RGD-K5 uptake changed from −81 % to −8 % (mean: −40 %, $p=0.005$) for the main tumor and from −85 % to +17 % (mean: −28 %, $p=0.069$) for nodes. The observed decrease in main tumor or nodal RGD-K5 uptake did not predict complete remission in the main tumor (−42 % versus −36 %, $p=0.697$) or in nodes (−34 % versus −22 %, $p=0.639$).

CCRT-induced changes in FDG uptake

At 2 weeks post-treatment, the FDG uptake did not differ significantly between complete responders and non-responders (main tumor SUV: 6.2 versus 4.9, respectively, $p=0.193$; lymph nodes SUV: 4.0 versus 5.8, respectively, $p=0.294$). Compared with baseline, the FDG uptake varied from −78 % to +42 % (mean: −58 %, $p=0.003$) for the main tumor and from −85 % to +91 % (mean: −42 %, $p=0.017$) for nodes. The observed decrease did not differ significantly between complete responders and non-responders (main tumor: −55 % versus −65 %, $p=0.529$; nodes: −38 % versus −49 %, $p=0.770$, respectively).

At the 3-month post-treatment scan, the FDG uptake at the main tumors was significantly higher in those with persistent tumor than in those without (mean SUV: 7.7 versus 4.1, respectively, $p=0.029$); the estimated power achieved 64.4 % under significance level 0.05. Compared with baseline, the main tumor FDG uptake varied from −87 % to −33 % (mean: −66 %, $p=0.005$). The observed decrease was lower in patients who had persistent main tumors than in those who did not, albeit not significantly so (−46 % versus −71 %, $p=0.118$). The nodal FDG uptake varied from −87 % to +13 % (mean: −51 %, $p=0.025$). Neither the decrease of nodal uptake nor the mean SUV predicted nodal response (−62 % *versus* −46 %, $p=0.733$; 2.9 versus 6.2, $p=0.172$, respectively).

Relationships between RDG-K5 and FDG uptake

We did not find significant associations between RDG-K5 and FDG uptake at baseline or 2-week post-treatment scans at

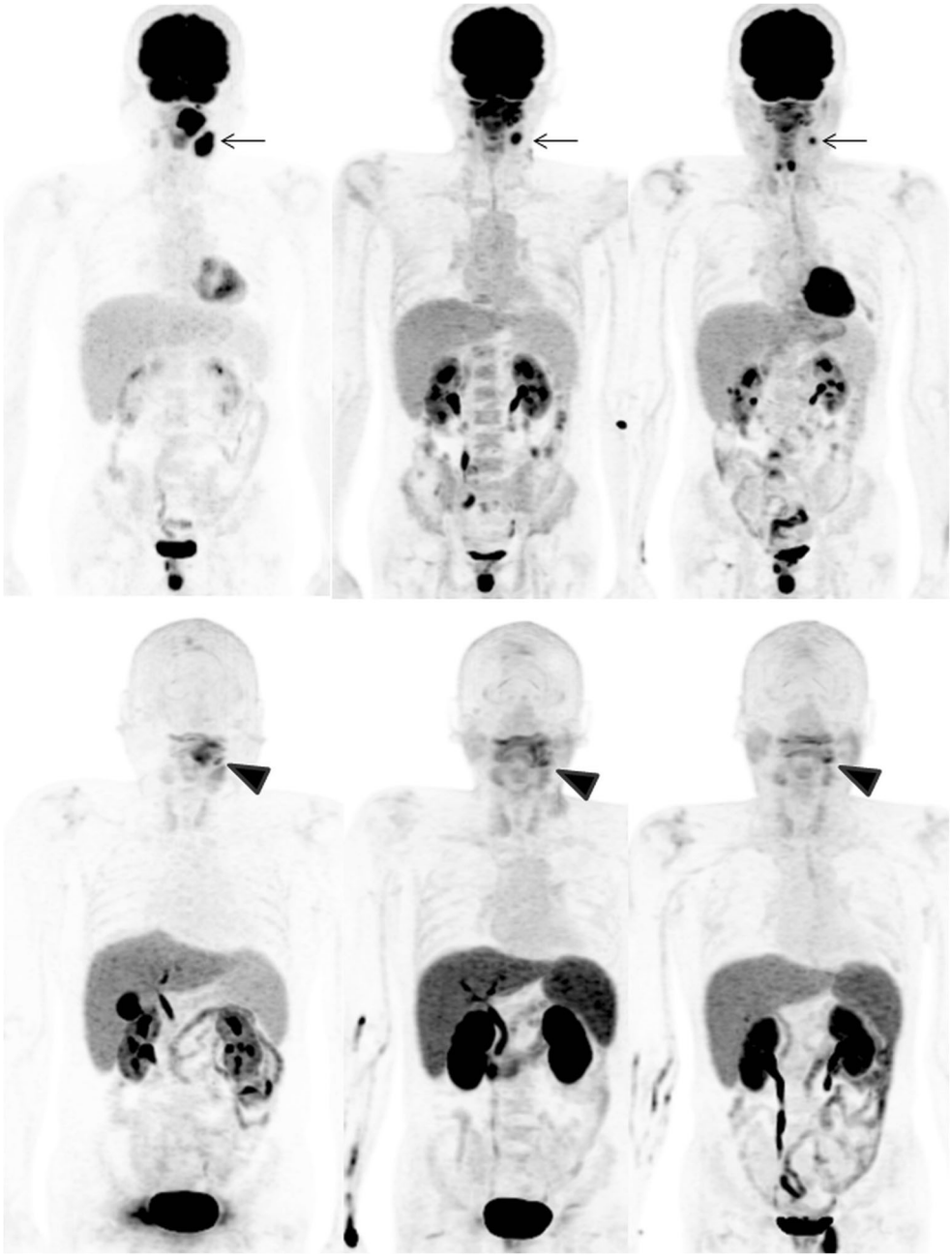

Fig. 2 Maximal intensity projection images of a patient who had persistent neck lymph node disease confirmed by biopsy and who underwent an additional neck dissection after chemoradiotherapy. Upper and lower row images represent the FDG and RGD-K5 scans, respectively, at baseline, 2 weeks, and 3 months after radiotherapy. A persistent left lymph node was evident on FDG imaging (arrow), but undetectable on RGD-K5. We noted the occurrence of RGD-K5 uptake on a tooth (arrowhead)

Table 2 Main tumor and nodal SUVmax of RGD-K5 and FDG according to treatment outcomes

Disease Control	baseline				2-week post-treatment scan				3-month post-treatment scan			
	RGD-K5		FDG		RGD-K5		FDG		RGD-K5		FDG	
	T	N	T	N	T	N	T	N	T	N	T	N
Yes (n)	5.6 (5)	4.7 (4)	15.1 (5)	12.3 (4)	3.2 (5)	2.3 (4)	6.3 (5)	3.2 (4)	2.3 (4)	2.1 (3)	3.4 (4)	2.7 (3)
No (n)	5.1 (7)	3.7 (6)	15.9 (7)	11.2 (6)	4.3 (7)	2.6 (6)	5.6 (7)	5.8 (6)	3.2 (6)	2.4 (5)	5.7 (6)	5.7 (5)
P value	0.746	0.566	0.753	0.782	0.139	0.427	0.491	0.126	**0.023**	0.512	0.108	0.236

Abbreviations: CCRT, concurrent chemoradiotherapy; T, main tumor; N, nodes

Table 3 Main tumor and nodal SUVmax of RGD-K5 and FDG according to the presence of main tumor recurrence

Main tumor recurrence	baseline				2-week post-treatment scan				3-month post-treatment scan			
	RGD-K5		FDG		RGD-K5		FDG		RGD-K5		FDG	
	T	N	T	N	T	N	T	N	T	N	T	N
Yes (n)	6.0 (3)	4.1 (2)	14.6 (3)	5.7 (2)	4.7 (3)	1.9 (2)	4.9 (3)	3.7 (2)	3.9 (2)	2.1 (1)	7.7 (2)	3.4 (1)
No (n)	5.1 (9)	4.1 (8)	15.9 (9)	13.1 (8)	3.6 (9)	2.6 (8)	6.2 (9)	5.0 (8)	2.6 (8)	2.3 (7)	4.1 (8)	4.7 (7)
P value	0.602	0.975	0.674	0.075	0.163	0.142	0.193	0.557	**0.007**	0.784	**0.029**	0.739

Abbreviations: CCRT, concurrent chemoradiotherapy; T, main tumor; N, nodes

either the main tumor (Spearman's $\rho = -0.007$, $p = 0.983$ at baseline; Spearman's $\rho = 0.119$, $p = 0.713$ at 2-week post-treatment) or lymph nodes (Spearman's $\rho = -0.200$, $p = 0.580$ at baseline; Spearman's $\rho = 0.468$, $p = 0.172$ at 2-week post-treatment). However, the uptake of RGD-K5 and FDG at the main tumors was significantly correlated with each other at 3 months post-treatment (Spearman's $\rho = 0.842$, $p = 0.002$). The uptake of lymph nodes was not correlated (Spearman's $\rho = 0.455$, $p = 0.257$). Similarly, the reductions of RDG-K5 and FDG uptake did not show reciprocal correlations at 2-week post-treatment (main tumor: Spearman's $\rho = 0.007$, $p = 0.983$; nodes: Spearman's $\rho = .188$, $p = 0.603$) or 3-month post-treatment scans (main tumor: Spearman's $\rho = 0.139$, $p = 0.701$; nodes: Spearman's $\rho = 0.143$, $p = 0.736$).

In general, the reduction of RGD-K5 uptake in the main tumor was less than that of FDG (2 weeks post-treatment: −13 % versus −58 %, respectively, $p = 0.015$; 3 months post-treatment: −40 % *versus* −66 %, $p = 0.028$, respectively); the estimated power achieved 70.8 % under significance level 0.05. However, the reduction of nodal RGD-K5 and FDG uptake did not differ significantly (2 weeks post-treatment: −27 % versus −42 %, $p = 0.386$; 3 months post-treatment: −28 % versus −51 %, $p = 0.123$, respectively).

Discussion

The primary hypothesis motivating the current study was that RGD-K5 (an integrin $\alpha\nu\beta3$ tracer) would be more specific than FDG for identifying lesions that did not respond to CCRT on PET images. Using a single-photon-emission computer tomography integrin $\alpha\nu\beta3$ tracer (In-111-RGD2) in a xenograft model of head and neck cancer, Terry et al. reported a decreased uptake occurring as early as 4 h after CCRT. The authors suggested the potential clinical utility of the integrin $\alpha\nu\beta3$ PET tracer for monitoring the early anti-angiogenic response elicited by CCRT [11]. In another study, Rylova et al. used a different integrin $\alpha\nu\beta3$ tracer [Ga-68-NODAGA-c(RGDfK)] for imaging FaDu xenograft (human hypopharyngeal squamous cell carcinoma cell line)-bearing mice treated with bevacizumab. The results indicated that 1) bevacizumab was unable to inhibit tumor growth and 2) no significant changes in Ga-68- NODAGA-c (RGDfK) uptake occurred [12]. Integrin $\alpha\nu\beta3$ has been implicated in both the angiogenic response induced by vascular endothelium growth factor (VEGF) and in cellular mobility [13, 14]. Abdollahi et al. [15] reported an upregulation of integrin $\alpha\nu\beta3$ in endothelial cells following CCRT, a phenomenon accompanied by Akt phosphorylation and activation of downstream survival pathways. Therefore, an increased RGD-K5 uptake in PET scans might be associated with radiation resistance, potentially being useful for the prediction of therapeutic failure.

Here, we performed a longitudinal analysis of RGD-K5 uptake over 3 months in patients with advanced head and neck cancer, with the goal of investigating its changes during the course of CCRT. The addition of a scan at 2 weeks after treatment was aimed at detecting abnormalities earlier than the traditional evaluation schedule (3 months after treatment).

Table 4 Main tumor and nodal SUVmax of RGD-K5 and FDG according to the presence of nodal recurrence

Nodal recurrence	baseline				2-week post-treatment scan				3-month post-treatment scan			
	RGD-K5		FDG		RGD-K5		FDG		RGD-K5		FDG	
	T	N	T	N	T	N	T	N	T	N	T	N
Yes (n)	5.3 (4)	3.3 (4)	14.7 (4)	12.7 (4)	3.9 (4)	2.8 (4)	6.2 (4)	5.8 (4)	3.1 (4)	2.6 (4)	5.6 (4)	6.2 (4)
No (n)	5.3 (8)	4.6 (6)	16.0 (8)	11.0 (6)	3.8 (8)	2.3 (6)	5.8 (8)	4.0 (6)	2.7 (6)	2.0 (4)	4.3 (6)	2.9 (4)
P value	0.979	0.455	0.656	0.647	0.892	0.227	0.672	0.294	0.429	0.293	0.410	0.172

Abbreviations: CCRT, concurrent chemoradiotherapy; T, main tumor; N, nodes

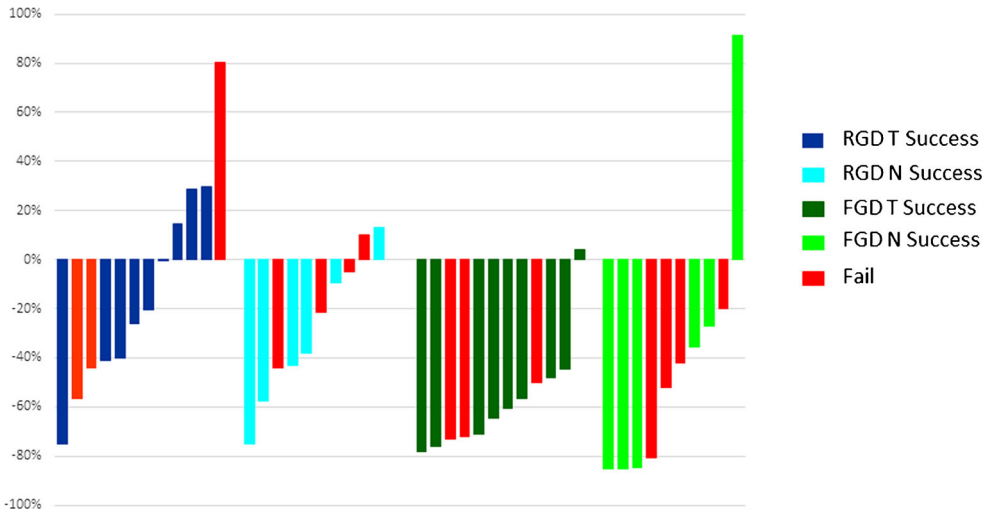

Fig. 3 Changes in standardized uptake value of RGD-K5 and FDG at the 2-week post-treatment scans compared with baseline

We have previously shown that an additional FDG-PET scan before adjuvant radiotherapy or concurrent chemoradiotherapy can improve patient outcomes [16, 17]. We thus hypothesized that an additional scan after radiotherapy could also be helpful. The results indicated that RGD-K5 uptake was generally less intense than that of FDG. In addition, CCRT-induced uptake changes were less prominent for RGD-K5 than FDG, albeit not significantly so at the nodal sites. We demonstrated that neither baseline RGD-K5 nor FDG uptake values, nor their CCRT-induced changes over time, were able to differentiate patients who successfully responded to CCRT from those who did not. Only at 3 months post-treatment, was the uptake of both RGD-K5 and FDG at main tumors significantly lower in those achieved complete response than those with residual tumors (Fig. 5). Although FDG-PET remains the most commonly used PET tracer for both tumor staging and the assessment of treatment response, false-positive results caused by inflammatory reactions continue to pose significant diagnostic challenges in the post-CCRT phase [18]. In this setting, new tracers capable of improving the prediction of treatment outcomes are eagerly awaited [19]. Our preliminary data suggest the potential usefulness of RGD-K5 to achieve this goal; however, larger studies are necessary to clarify whether RGD-K5 is superior to FDG.

As CCRT-induced DNA damage is dependent on oxygen for the formation of free radicals, hypoxia has been associated with a reduced CCRT effectiveness [20]. Moreover, hypoxic head and neck tumors portend a poor prognosis [21]. VEGF, an important mediator of angiogenesis, is induced under hypoxic conditions through the hypoxia-inducible factor-1α (HIF-1α) pathway [22]. An increased VEGF expression carries adverse prognostic significance in patients with head and neck cancer [23]. Consistent evidence also indicates that radiation may activate different angiogenesis-related pathways, including phosphatidylinositol-3-kinase (PI3-K)/protein kinase B [24], HIF-1α [25], and VEGF [26], ultimately

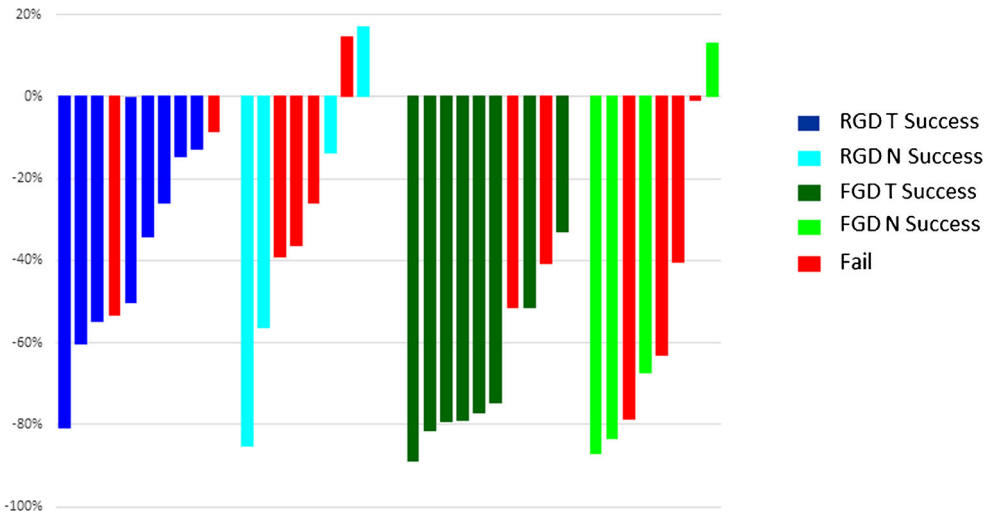

Fig. 4 Changes in the standardized uptake value of RGD-K5 and FDG at the 3-month post-treatment scans compared with baseline

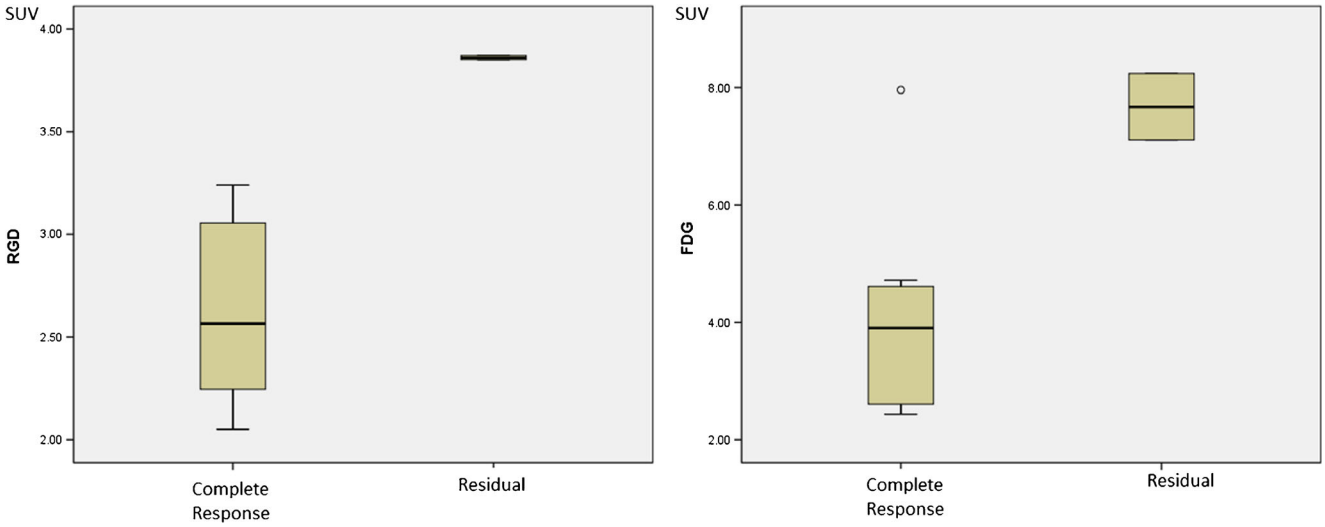

Fig. 5 SUV of RGD-K5 and FDG at main tumors at 3 months post-treatment

promoting the formation of new vessels [27]. In this scenario, the combination of anti-angiogenic strategies with CCRT has been proposed as a valuable approach to overcome radiation resistance. Results from phase II trials combining bevacizumab and chemotherapy and/or epidermal growth factor receptor antagonists in patients with head and neck malignancies have been promising [28–35]. Phase III trials of anti-angiogenic drugs (e.g., bevacizumab, afatinib) in this patient group are currently ongoing (clinicaltrials.gov identifiers NCT00588770, NCT01345669). However, a phase II study of cilengitide (an integrin $\alpha v\beta 3$ and $\alpha v\beta 5$ inhibitor) combined with cisplatin, 5-fluorouracil, and cetuximab failed to show significant benefits in terms of progression-free survival for patients with recurrent/metastatic head and neck cancer [36]. Although the evidence supporting the use of anti-angiogenic drugs in combination with CCRT remains weak, further studies are necessary to investigate the potential usefulness of RGD-K5 PET imaging for monitoring response to drugs specifically targeting angiogenesis.

In summary, the results of this pilot study demonstrate that only at 3 months post-treatment, the uptake of both RGD-K5 and FDG at main tumors had the ability to discriminate patients who were successfully treated from those with residual disease. Albeit preliminary and subject to future confirmation in larger studies, our findings support the potential usefulness of RGD-K5 for assessing the response to CCRT in patients with advanced HNC.

Acknowledgments The study was supported by a grant from the Chang Gung Memorial Hospital CMRPG3A0781-3 and was performed using the equipment of the Center for Advanced Molecular Imaging and Translation.

The precursor of RGD-K5 was kindly provided by Siemens Molecular Imaging, Inc.

Compliance with ethical standards All procedures performed in studies involving human participants were in accordance with the ethical standards of the institutional and/or national research committee and with the 1964 Helsinki declaration and its later amendments or comparable ethical standards.

References

1. Hanahan D, Weinberg RA. Hallmarks of cancer: the next generation. Cell. 2011;144(5):646–74. doi:10.1016/j.cell.2011.02.013.
2. Desgrosellier JS, Cheresh DA. Integrins in cancer: biological implications and therapeutic opportunities. Nat Rev Cancer. 2010;10(1):9–22. doi:10.1038/nrc2748.
3. Fabricius EM, Wildner GP, Kruse-Boitschenko U, Hoffmeister B, Goodman SL, Raguse JD. Immunohistochemical analysis of integrins alphavbeta3, alphavbeta5 and alpha5beta1, and their ligands, fibrinogen, fibronectin, osteopontin and vitronectin, in frozen sections of human oral head and neck squamous cell carcinomas. Exp Ther Med. 2011;2(1):9–19. doi:10.3892/etm.2010.171.
4. Beer AJ, Haubner R, Sarbia M, Goebel M, Luderschmidt S, Grosu AL, et al. Positron emission tomography using [18F]Galacto-RGD identifies the level of integrin alpha(v)beta3 expression in man. Clin Cancer Res. 2006;12(13):3942–9. doi:10.1158/1078-0432.CCR-06-0266.
5. Beer AJ, Grosu AL, Carlsen J, Kolk A, Sarbia M, Stangier I, et al. [18F]galacto-RGD positron emission tomography for imaging of alphavbeta3 expression on the neovasculature in patients with squamous cell carcinoma of the head and neck. Clin Cancer Res. 2007;13(22 Pt 1):6610–6. doi:10.1158/1078-0432.CCR-07-0528.
6. Hsu HW, Wall NR, Hsueh CT, Kim S, Ferris RL, Chen CS, et al. Combination antiangiogenic therapy and radiation in head and neck cancers. Oral Oncol. 2014;50(1):19–26. doi:10.1016/j.oraloncology.2013.10.003.
7. Sahu N, Grandis JR. New advances in molecular approaches to head and neck squamous cell carcinoma. Anti-Cancer Drugs. 2011;22(7):656–64. doi:10.1097/CAD.0b013e32834249ba.
8. Doss M, Kolb HC, Zhang JJ, Belanger MJ, Stubbs JB, Stabin MG, et al. Biodistribution and radiation dosimetry of the integrin marker 18F-RGD-K5 determined from whole-body PET/CT in monkeys and humans. J Nucl Med. 2012;53(5):787–95. doi:10.2967/jnumed.111.088955.
9. Wang HM, Hsu CL, Hsieh CH, Fan KH, Lin CY, Chang JT, et al. Concurrent chemoradiotherapy using cisplatin, tegafur, and

leucovorin for advanced squamous cell carcinoma of the hypopharynx and oropharynx. Biomed J. 2014;37(3):133–40. doi:10.4103/2319-4170.117893.
10. Faul F, Erdfelder E, Buchner A, Lang AG. Statistical power analyses using G*Power 3.1: Tests for correlation and regression analyses. Behav Res Methods. 2009;41(4):1149–60. doi:10.3758/BRM.41.4.1149.
11. Terry SY, Abiraj K, Lok J, Gerrits D, Franssen GM, Oyen WJ, et al. Can 111In-RGD2 monitor response to therapy in head and neck tumor xenografts? J Nucl Med. 2014;55(11):1849–55. doi:10.2967/jnumed.114.144394.
12. Rylova SN, Barnucz E, Fani M, Braun F, Werner M, Lassmann S, et al. Does imaging alphavbeta3 integrin expression with PET detect changes in angiogenesis during bevacizumab therapy? J Nucl Med. 2014;55(11):1878–84. doi:10.2967/jnumed.114.137570.
13. Chuang JY, Chang AC, Chiang IP, Tsai MH, Tang CH. Apoptosis signal-regulating kinase 1 is involved in WISP-1-promoted cell motility in human oral squamous cell carcinoma cells. PLoS One. 2013;8(10):e78022. doi:10.1371/journal.pone.0078022.
14. Chuang JY, Chen PC, Tsao CW, Chang AC, Lein MY, Lin CC, et al. WISP-1 a novel angiogenic regulator of the CCN family promotes oral squamous cell carcinoma angiogenesis through VEGF-A expression. Oncotarget. 2015;6(6):4239–52.
15. Abdollahi A, Griggs DW, Zieher H, Roth A, Lipson KE, Saffrich R, et al. Inhibition of alpha(v)beta3 integrin survival signaling enhances antiangiogenic and antitumor effects of radiotherapy. Clin Cancer Res. 2005;11(17):6270–9. doi:10.1158/1078-0432.CCR-04-1223.
16. Liao CT, Fan KH, Lin CY, Wang HM, Huang SF, Chen IH, et al. Impact of a second FDG PET scan before adjuvant therapy for the early detection of residual/relapsing tumours in high-risk patients with oral cavity cancer and pathological extracapsular spread. Eur J Nucl Med Mol Imaging. 2012;39(6):944–55. doi:10.1007/s00259-012-2103-2.
17. Kang CJ, Lin CY, Yang LY, Ho TY, Lee LY, Fan KH, et al. Positive clinical impact of an additional PET/CT scan before adjuvant radiotherapy or concurrent chemoradiotherapy in patients with advanced oral cavity squamous cell carcinoma. J Nucl Med. 2015;56(1):22–30. doi:10.2967/jnumed.114.145300.
18. Prestwich RJ, Subesinghe M, Gilbert A, Chowdhury FU, Sen M, Scarsbrook AF. Delayed response assessment with FDG-PET-CT following (chemo) radiotherapy for locally advanced head and neck squamous cell carcinoma. Clin Radiol. 2012;67(10):966–75. doi:10.1016/j.crad.2012.02.016.
19. Ul-Hassan F, Simo R, Guerrero-Urbano T, Oakley R, Jeannon JP, Cook GJ. Can (18)F-FDG PET/CT reliably assess response to primary treatment of head and neck cancer? Clin Nucl Med. 2013;38(4):263–5. doi:10.1097/RLU.0b013e31828165a8.
20. Karar J, Maity A. Modulating the tumor microenvironment to increase radiation responsiveness. Cancer Biol Ther. 2009;8(21):1994–2001.
21. Toustrup K, Sorensen BS, Nordsmark M, Busk M, Wiuf C, Alsner J, et al. Development of a hypoxia gene expression classifier with predictive impact for hypoxic modification of radiotherapy in head and neck cancer. Cancer Res. 2011;71(17):5923–31. doi:10.1158/0008-5472.CAN-11-1182.
22. Vassilakopoulou M, Psyrri A, Argiris A. Targeting angiogenesis in head and neck cancer. Oral Oncol. 2015;51(5):409–15. doi:10.1016/j.oraloncology.2015.01.006.
23. Kyzas PA, Cunha IW, Ioannidis JP. Prognostic significance of vascular endothelial growth factor immunohistochemical expression in head and neck squamous cell carcinoma: a meta-analysis. Clin Cancer Res. 2005;11(4):1434–40. doi:10.1158/1078-0432.CCR-04-1870.
24. Bussink J, van der Kogel AJ, Kaanders JH. Activation of the PI3-K/AKT pathway and implications for radioresistance mechanisms in head and neck cancer. Lancet Oncol. 2008;9(3):288–96. doi:10.1016/S1470-2045(08)70073-1.
25. Moeller BJ, Cao Y, Li CY, Dewhirst MW. Radiation activates HIF-1 to regulate vascular radiosensitivity in tumors: role of reoxygenation, free radicals, and stress granules. Cancer Cell. 2004;5(5):429–41.
26. Sofia Vala I, Martins LR, Imaizumi N, Nunes RJ, Rino J, Kuonen F, et al. Low doses of ionizing radiation promote tumor growth and metastasis by enhancing angiogenesis. PLoS One. 2010;5(6):e11222. doi:10.1371/journal.pone.0011222.
27. Bozec A, Sudaka A, Fischel JL, Brunstein MC, Etienne-Grimaldi MC, Milano G. Combined effects of bevacizumab with erlotinib and irradiation: a preclinical study on a head and neck cancer orthotopic model. Br J Cancer. 2008;99(1):93–9. doi:10.1038/sj.bjc.6604429.
28. Cohen EE, Davis DW, Karrison TG, Seiwert TY, Wong SJ, Nattam S, et al. Erlotinib and bevacizumab in patients with recurrent or metastatic squamous-cell carcinoma of the head and neck: a phase I/II study. Lancet Oncol. 2009;10(3):247–57. doi:10.1016/S1470-2045(09)70002-6.
29. Argiris A, Karamouzis MV, Gooding WE, Branstetter BF, Zhong S, Raez LE, et al. Phase II trial of pemetrexed and bevacizumab in patients with recurrent or metastatic head and neck cancer. J Clin Oncol. 2011;29(9):1140–5. doi:10.1200/JCO.2010.33.3591.
30. Hainsworth JD, Spigel DR, Greco FA, Shipley DL, Peyton J, Rubin M, et al. Combined modality treatment with chemotherapy, radiation therapy, bevacizumab, and erlotinib in patients with locally advanced squamous carcinoma of the head and neck: a phase II trial of the Sarah Cannon oncology research consortium. Cancer J. 2011;17(5):267–72. doi:10.1097/PPO.0b013e3182329791.
31. Yoo DS, Kirkpatrick JP, Craciunescu O, Broadwater G, Peterson BL, Carroll MD, et al. Prospective trial of synchronous bevacizumab, erlotinib, and concurrent chemoradiation in locally advanced head and neck cancer. Clin Cancer Res. 2012;18(5):1404–14. doi:10.1158/1078-0432.CCR-11-1982.
32. Argiris A, Kotsakis AP, Hoang T, Worden FP, Savvides P, Gibson MK, et al. Cetuximab and bevacizumab: preclinical data and phase II trial in recurrent or metastatic squamous cell carcinoma of the head and neck. Ann Oncol. 2013;24(1):220–5. doi:10.1093/annonc/mds245.
33. Fury MG, Lee NY, Sherman E, Lisa D, Kelly K, Lipson B, et al. A phase 2 study of bevacizumab with cisplatin plus intensity-modulated radiation therapy for stage III/IVB head and neck squamous cell cancer. Cancer. 2012;118(20):5008–14. doi:10.1002/cncr.27498.
34. Yao M, Galanopoulos N, Lavertu P, Fu P, Gibson M, Argiris A, et al. Phase II study of bevacizumab in combination with docetaxel and radiation in locally advanced squamous cell carcinoma of the head and neck. Head Neck. 2015;37(11):1665–71. doi:10.1002/hed.23813.
35. Fury MG, Xiao H, Sherman EJ, Baxi S, Smith-Marrone S, Schupak K, et al. Phase II trial of bevacizumab + cetuximab + cisplatin with concurrent intensity-modulated radiation therapy for patients with stage III/IVB head and neck squamous cell carcinoma. Head Neck. 2015. doi:10.1002/hed.24041.
36. Vermorken JB, Peyrade F, Krauss J, Mesia R, Remenar E, Gauler TC, et al. Cisplatin, 5-fluorouracil, and cetuximab (PFE) with or without cilengitide in recurrent/metastatic squamous cell carcinoma of the head and neck: results of the randomized phase I/II ADVANTAGE trial (phase II part). Ann Oncol. 2014;25(3):682–8. doi:10.1093/annonc/mdu003.